



Surface chemistry and reactivity of ceria–zirconia-supported palladium oxide catalysts for natural gas combustion

Stefania Specchia^{a,*}, Elisabetta Finocchio^b, Guido Busca^b, Pietro Palmisano^a, Vito Specchia^a

^a Catalytic Reaction Engineering for Energy and Environment (CRE³) Group, Dipartimento di Scienza dei Materiali e Ingegneria Chimica, Politecnico di Torino, Corso Duca degli Abruzzi 24, I-10129 Torino, Italy

^b Laboratorio di Chimica delle Superfici e Catalisi Industriale, Dipartimento di Ingegneria Chimica e di Processo, Università di Genova, Piazzale Kennedy 1, I-16129 Genova, Italy

ARTICLE INFO

Article history:

Received 7 November 2008

Revised 15 January 2009

Accepted 2 February 2009

Available online 20 February 2009

Keywords:

Palladium oxide

Nanoparticles

IR spectroscopy

Adsorbed CO

Supported Pd catalysts

Ceria–zirconia catalyst supports

CH₄ catalytic combustion

Ageing mechanism

SO₂ poisoning

ABSTRACT

The behavior of 2% Pd catalyst supported on ceria–zirconia, prepared by solution combustion synthesis, was investigated in fresh and aged status, after severe hydro-thermal ageing in presence of SO₂. A surface chemical characterization study was performed using methane temperature programmed combustion, oxygen temperature-programmed desorption, hydrogen temperature-programmed reduction and infrared spectroscopy of low temperature carbon monoxide adsorption. The fresh catalyst is mostly constituted by partly oxidized very small Pd metal particles and dispersed Pd oxide species. This situation gives rise to high catalytic activity for methane combustion at low temperature. The progressive oxidation of highly dispersed small Pd particles to PdO_x, as well as the coalescence of dispersed Pd oxide species result in PdO_x particles fully oxidized at least at the surface which are less active (in the low temperature range) with respect to the active species of the original catalyst.

© 2009 Elsevier Inc. All rights reserved.

1. Introduction

Premixed natural gas combustion within porous media coupled with a catalytic system was found to represent an excellent solution for energy production for domestic applications [1–6]: as main obtained results up to today, a considerable reduction of CO and unburned hydrocarbons, coupled with a limited production of thermal NO_x, can be listed, together with an enhanced overall thermal efficiency.

Palladium based catalysts appear to be the most active catalysts for natural gas combustion [7,8]. Alumina is the most largely used support, although addition of ceria is reported to be beneficial [9–12]. Zirconia supported catalysts have also been investigated [13–18]. Dispersing a noble metal over a support intrinsically active towards catalytic oxidation, such as CeO₂–ZrO₂ mixed oxides, was expected to have favorable effects on the overall catalytic activity. Apart as catalyst for CH₄ combustion [15,19–21], Pd/CeO₂–ZrO₂ systems are also known in literature as very good and promising catalysts for other industrial applications, such as three-way catalysts (TWC) for automotive applications [22–29], or catalysts for diesel soot combustion [30–32], NO reduction by CO

[33–35], methanol decomposition into syngas [36], toluene combustion [37].

Despite there are still some divergences in literature concerning mainly which is the most active state of the Pd-based catalysts for CH₄ oxidation (metallic Pd [38–42], PdO [7,43–48] or a mixed phase Pd⁰/PdO_x [49–51]), the Pd active phase as oxidation catalysts is mostly identified as PdO [43,44], which is known to decompose into Pd metal in the range 650–850 °C, depending on O₂ partial pressure [52,53] and reactive gas mixture composition. The transformation of PdO into Pd is reported to negatively affect catalytic reaction by lowering conversion; anyway, CH₄ combustion activity has been reversibly restored upon re-oxidation of Pd to PdO. The nature of the support is reported to influence strongly the re-oxidation of Pd metal, which is in particular favored by addition of CeO₂ to both Al₂O₃ [10,12,54] and ZrO₂ [55–57] supports.

Vibrational spectroscopic studies of adsorbed CO represent, since decades, very informative investigations on the surface state of bulk and supported metal catalysts [58,59]. Infrared studies of CO adsorption at low temperature are largely applied to the characterization of the oxidation and coordination state of cationic metal centers on oxide surfaces [60,61]. Application of these techniques to real Pd oxide based oxidation catalysts is, however, quite scarce [62–64]. The existence of species different from Pd and PdO massive particles, such as dispersed Pd⁺, Pd²⁺ and Pd⁴⁺ species, has been proposed on the frame of these investigations. On the

* Corresponding author. Fax: +39 011 0904699.

E-mail address: stefania.specchia@polito.it (S. Specchia).

other hand, recent surface science studies with innovative techniques performed on model “planar” catalysts [65] as well as theoretical investigations [66] have provided additional detailed information on the oxidation catalysis over Pd catalysts.

In the present paper a surface chemical characterization study of CeO₂–ZrO₂ supported 2% Pd catalyst, hereafter named PCZ, is reported. Such a catalyst was developed for natural gas combustion in premixed burners as a source of thermal energy in domestic appliances (heating and sanitary water production), and found excellent activity [5,6,67]. The aim is to investigate the details of the catalytic active sites and the reasons of the deactivation behavior after prolonged treatment under hydrothermal ageing conditions and sulfur compounds poisoning.

2. Experimental

Two Pd/ γ -Al₂O₃ catalysts were used as reference materials. Sample PA1 was prepared from Degussa Aluminum oxide C (10% Pd, 100 m² g⁻¹; mean particle size 55 μ m, crystallite size 13 nm) by impregnation with Pd(NO₃)₂·2H₂O, subsequent drying at 80 °C for 48 h and calcination at 450 °C for 3 h. Sample PA2 was prepared using Pural SB alumina from Condea (2.7% Pd, 193 m² g⁻¹; mean particle size: 45 μ m, crystallite size 5 nm) with a similar impregnation procedure.

2% Pd on CeO₂–ZrO₂ (PCZ) powdered catalysts were prepared via solution combustion synthesis (SCS) [6,67–69]. Ce, Pd and ZrO nitrates (Aldrich, 99% purity) were used as precursors, the nitrate ion acting as oxidizer of glycine in solution. The organic molecule guarantees good solution homogeneity, preventing the preferential precipitation of ionic species, and reacts with the precursors (metal nitrates). The precursors and glycine, dosed in the stoichiometric amounts, were dissolved in distilled water and the resulting solution, thoroughly stirred to ensure complete dissolution of all reagents, was then transferred in a ceramic dish and placed into an electric oven set at 450 °C. After water evaporation and a significant increase in the system viscosity, the heat released in the fast reaction allowed the formation of the catalytic powders. Subsequently, the as-prepared powders were calcined in oven at 800 °C for 2 h in still air, so as to favor decomposition of the eventually unreacted nitrate precursor [6,67].

The catalytic activity towards CH₄ oxidation of the fresh and aged PCZ powders was tested in a lab-scale fixed-bed micro-reactor (temperature programmed combustion, TPC): 0.1 g of catalyst mixed with 0.9 g of SiO₂ (0.2–0.5 mm in size, to prevent the catalytic bed clogging), sandwiched between two quartz wool layers, were inserted in a quartz tube (4 mm ID). The obtained micro-reactor was placed into a PID regulated electrical oven and fed with 50 Ncm³ min⁻¹ of a gaseous mixture containing 2% CH₄ and 16% O₂ in He. The micro-reactor temperature was measured by a K-type thermocouple placed inside the catalytic bed. Starting from 800 °C, the oven temperature was decreased at 2 °C min⁻¹ rate and the outlet CO₂, CO, CH₄ and O₂ concentrations were determined by a continuous analyzer (NDIR and paramagnetic Uras 14, ABB), thus allowing to evaluate CH₄ conversion. The temperature where 50% conversion of CH₄ occurred, *T*₅₀, was considered as an index of the powders catalytic activity.

To evaluate the effect of time on stream, the catalytic powders were aged for different times with an “accelerated” ageing procedure. They were kept in an electric tubular oven at 800 °C (a thermocouple was used to monitor the furnace temperature) under a flow rate with typical domestic boiler exhaust composition (9% CO₂, 18% H₂O, 2% O₂ in N₂); 200 ppmv of SO₂ were added too [6,67]. The latter value was chosen several times higher than the odorant supplementary concentration in commercial natural gas (in Italy, about 8 ppmv of tetrahydrothiophene, C₄H₈-S, also known as THT) so as to accelerate any possible poisoning effect. Earlier

sulfur poisoning studies on perovskite catalysts showed that the basic poisoning mechanism under catalytic combustion conditions was chemisorption of SO₂/SO₃ species generated by combustion of whatever sulfur-organic compound present in the feed (e.g., odorants) [70]. Particularly, it was demonstrated that the direct presence of SO₂ or of the THT odorant in the feed did not lead to a significantly different ageing effect, provided the overall sulfur content remaining the same. SO₂/SO₃ species, in fact, resulted from the total oxidation of S-containing organics during the combustion process [71]. For this reason only ageing runs with a SO₂-laden flow were accomplished. The catalyzed burners were continuously aged up to 3 weeks: for a domestic boiler, such operating time in 200 ppmv SO₂ atmosphere may be considered equivalent to a utilization life time of approximately three years under real operation [67]. The as-prepared catalysts were completely characterized at fresh status and after each week of ageing (PCZ-F, PCZ-1W, PCZ-2W and PCZ-3W samples).

The crystallite phases size of the various catalysts were detected by X-ray diffraction (Philips PW1710 apparatus equipped with a monochromator for the CuK α radiation; markers located according the PcpdfWin database). The surface area and the pore size distribution of all samples were determined by N₂ adsorption at the liquid N₂ temperature in a Micrometrics ASAP 2010 M instrument. The surface area was determined according to the Brunauer–Emmett–Teller theory; the samples were degassed in vacuum for at least 4 h at 250 °C before analysis.

Temperature-programmed desorption (TPD) and temperature-programmed reduction (TPR) tests (Thermoquest TPD/R/O 1100 Series, Thermo Finningan analyzer, equipped with a thermal conductivity detector TCD) were employed to investigate the O₂ desorption with temperature and to quantify the presence of PdO on the catalysts’ surface on fresh and aged samples. To perform calculations on PdO amount, reference supports of pure CeO₂–ZrO₂ (CZ) without noble metal were also employed. TPR tests were performed by firstly flowing 10 Ncm³ min⁻¹ of 5% H₂ in Ar, increasing the temperature from 50 to 900 °C at 10 °C min⁻¹ to evaluate the H₂ consumption. Then an oxidation treatment was performed by flowing 40 Ncm³ min⁻¹ of pure O₂ increasing the temperature from 25 to 750 °C at 40 °C min⁻¹ followed by cooling to room temperature in the same oxidizing atmosphere. With the catalysts completed oxidized, TPR tests were performed again by flowing once more 10 Ncm³ min⁻¹ of 5% H₂ in Ar, increasing the temperature from 50 to 900 °C at 10 °C min⁻¹ to evaluate the new H₂ consumption. Mathematical calculations on the PdO_x percentage were accomplished by considering the initial and adsorbed volumes of gas, the catalyst amount and the noble metal percentage.

For IR studies, pressed disks of the pure catalysts powders were activated “in situ” by using an infrared cell connected to a conventional gas manipulation/outgassing ramp. All catalysts were first submitted to a treatment in air at 400 °C, for 30 min, followed by evacuation at the same temperature before the adsorption experiments. In order to obtain the reduced catalysts, after the mentioned evacuation, they were put in contact with a H₂ pressure \sim 300 Torr at 400 °C, for 30 min, and successively outgassed at the same temperature. CO adsorption was performed at –140 °C by the introduction of a known dose of the gas (10 Torr) inside the low temperature infrared cell containing the previously activated wafers. IR spectra were collected, evacuating at increasing temperatures between –140 and 0 °C. Spectra have been recorded in the temperature range –140 °C to room temperature by a Nicolet Nexus FT instrument.

3. Results

The XRD spectra for as-synthesized fresh and aged powders are presented in Fig. 1. The fresh sample crystallized as tetrago-

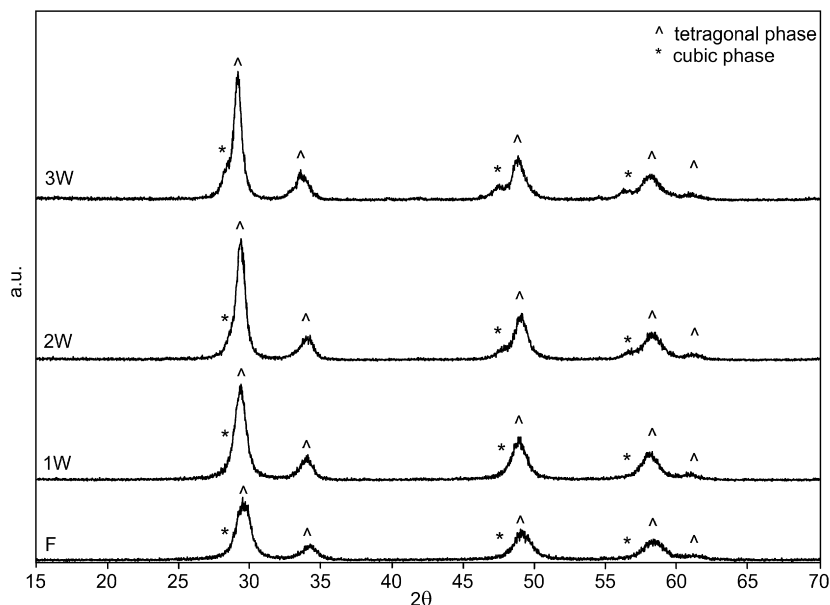


Fig. 1. XRD patterns of the fresh and aged PCZ catalysts.

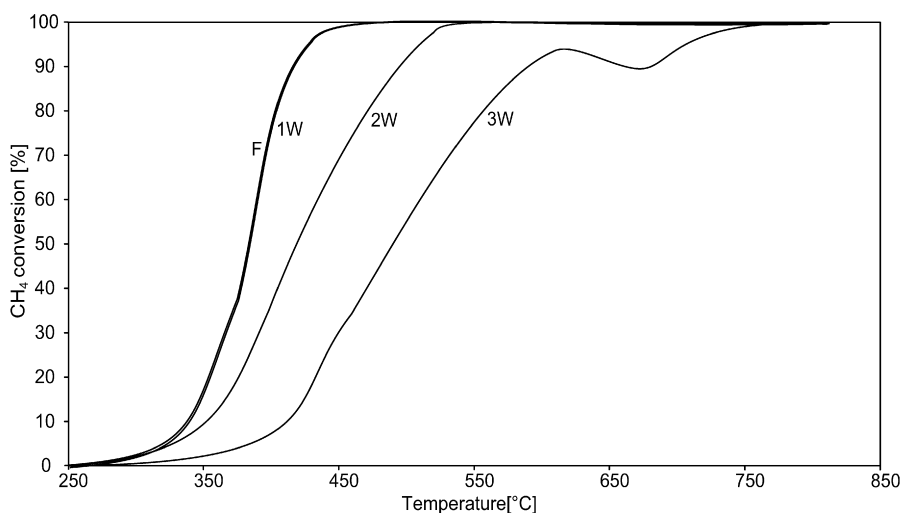


Fig. 2. CH₄ temperature-programmed combustion curves of the fresh and aged PCZ catalysts.

Table 1
Characteristics of the fresh and aged PCZ catalysts under study.

2% Pd/ CeO ₂ -ZrO ₂	BET (m ² g ⁻¹)	Crystallite size ^a (nm)	T ₅₀ (°C)	Desorbed O ₂ (μmol g ⁻¹)	PdO ^b (%)
PCZ-F	74.6	56	380	54.3	28.6
PCZ-1W	62.3	75	380	49.9	34.4
PCZ-2W	34.8	85	420	52.7	n.d.
PCZ-3W	21.5	96	490	51.9	82.6

^a Cubic phase.

^b From H₂ TPR data.
n.d.—not determined.

nal CeO₂-ZrO₂ solid solution phase (space group *P4₂/nmc*, *Z* = 2), in agreement with previous studies given the composition of our sample [72], while a cubic fluorite-like CeO₂ (or CeO₂-rich) phase (space group *Fm3m*, *Z* = 4) segregates out after 2 and 3 weeks ageing. The presence of eventual micro-domains of Ce-rich or Zr-rich phases cannot be detected by conventional diffraction analysis because the crystallographic structure and orientation of the atomic planes are the same for all CeO₂- and ZrO₂-enriched regions within the crystallite [27]. CO adsorption could discriminate between Ce and Zr ions, but apparently no surface enrichment can be evi-

denced in the present case. No diffraction peaks related to Pd or PdO were detected, in agreement with the small Pd loading.

The BET values, reported in Table 1 together with the mean crystallite size of the cubic phase calculated via the Scherrer equation, were very high (strongly related to the synthesis method that allows to process powder with high surface area). However, ageing resulted in a severe loss of surface area.

Fig. 2 shows the TPC results of fresh and aged PCZ catalysts. The catalyst performance remained stable till 1 week ageing, with a decline increasing with time on the 2W and 3W samples. It seems that the decline of catalytic activity is much less pronounced than the decline in total surface area of the catalyst. It seems also interesting to remark that, while reaction started at the same temperature for the PCZ-2W sample, only for the PCZ-3W sample the reaction started at a definitely higher temperature. On the other hand, the catalyst severely aged for three weeks actually retained catalytic activity with almost total CH₄ conversion at 600 °C. It seems also interesting that the CH₄ conversion on the 3W catalyst is more than 96% above 700 °C, it decreases a little bit until 90% at 650 °C, and increases again to about 93% at lower temperatures (600 °C) monotonically with decreasing temperature. A similar be-

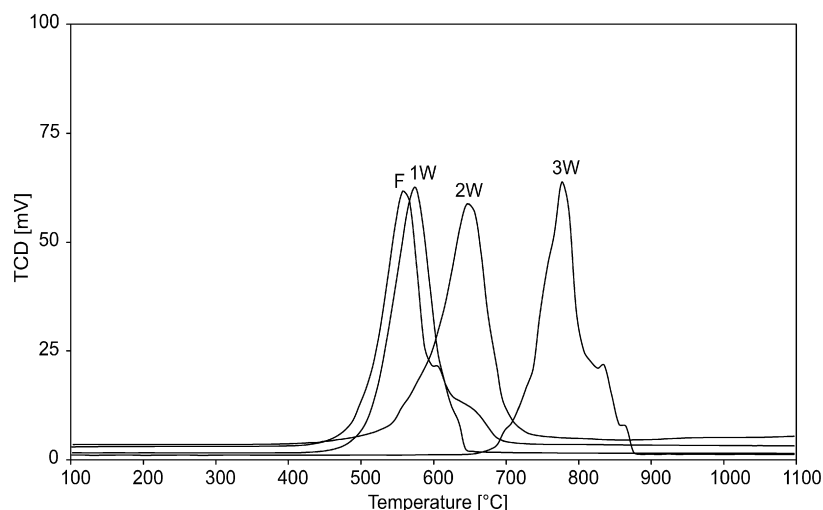


Fig. 3. O₂ temperature-programmed combustion curves of the fresh and aged PCZ catalysts.

havior, recorded in other cases during cooling [7,46,50,51], was found to be associated to the oxidation of Pd metal (the stable phase in low O₂ partial pressure and high temperature) to PdO, which would be more active in this temperature range.

The oxidation state of the fresh and the aged catalysts were studied by O₂ TPD (Fig. 3). The O₂ TPD curve of the fresh catalyst showed the desorption threshold near 430 °C, the peak near 560 °C and a further desorption tail in the region 600–700 °C. The peak temperature T_p was far higher than the temperature at which catalytic reaction started. In fact the O₂ desorption threshold temperature was practically coincident to the temperature at which CH₄ conversion became complete. The O₂ desorption temperatures from the fresh catalyst were far lower than those reported for decomposition of bulk PdO into Pd metal (730–830 °C) [43,44,52] but not too far from the temperature at which adsorbed O₂ was found to desorb from Pd(111) single crystal surface (490 °C) [73].

The catalyst maintained, after ageing, practically the same desorption performance in terms of amount of desorbed O₂ (average value: 52.2 μmol g⁻¹ ± 4.2%). The desorption threshold also remained the same after one and two weeks ageing, when, however, the peak maximum shifted to higher temperatures. This shift was very small after one week (to 580 °C), but significant after two weeks ageing (650 °C).

After three weeks ageing both desorption threshold and T_p shifted appreciably to higher values (650 °C and 790 °C, respectively), with the latter just in the region reported for PdO particles decomposition (730–830 °C) [43,44,52]. Also for the 3W sample, however, the desorption threshold temperature nearly coincided with that at which CH₄ conversion was complete in TPC experiments. The trends of T_{90} (CH₄ combustion TPC) and T_p (O₂ desorption TPD) are, in fact, in close agreement. The lower the O₂ desorption temperature range (see the T_p values), the higher the catalytic activity toward CH₄ combustion.

Being the amount of Pd loaded to the catalyst about 190 μmol g⁻¹, attributing all the O₂ evolved by the catalyst to the decomposition of (formally) PdO oxide species (thus excluding a direct participation of CeO₂ in O₂ desorption), it is possible to conclude that a little less than half Pd atoms remained indeed oxidized and/or could be reduced to Pd metal by thermal treatment. In other words, the averaged composition of surface “palladium oxide” species should have been near Pd₂O, supposing it to fully decompose into Pd metal upon TPD runs. Additionally, the amount of desorbed O₂ was independent from the total surface area of the sample. It seems consequently likely that, despite the sintering of the support, all the Pd species remained available at the sur-

face, allowing O₂ desorption. However, the nature of these species should change, with a resulting increase of the temperature of the O₂ TPD peak and a parallel decrease of the catalytic activity. In case of complete dispersion of Pd atoms at the surface of CZ, the density of Pd atoms should increase upon ageing from ~1.25 atom nm⁻² for the fresh catalyst up to ~5 atom nm⁻² for the 3W aged sample. Therefore, on the 3W aged sample each Pd atom had still available ~20 Å², thus having the possibility (geometrically speaking) to remain atomically dispersed also after the carrier sintering upon ageing.

TPR results are reported in Table 1 as percentage of reducible Pd oxide species (assuming the PdO stoichiometry) present on each catalytic sample: it increased upon ageing and deactivation. It is worthy to note that the amount of O₂ calculated from TPD and TPR data is different but in the same order of magnitude, suggesting that different types of Pd oxides may exist. Moreover, TPR peaks came out approx at the same temperature, without separation among them; the only difference is related to the peaks' intensity: the more aged the catalyst, the more hydrogen is consumed. Although also sulfates species could consume H₂, it is worth note that Pd is predominant.

In Fig. 4 the IR spectra of pressed disks of the fresh and the 2 weeks aged PCZ catalysts are compared with those of the support treated in the same way. The fresh support shows a broad but well defined OH stretching band at 3670 cm⁻¹ with a shoulder at 3710 cm⁻¹ providing evidence of surface hydroxy groups. The position of these components corresponds to those of some OH's observed on ZrO₂ polymorphs (3670 cm⁻¹) [59,74], with that of OH groups observed on CeO₂ (3710 cm⁻¹) [59] suggesting that such hydroxy groups may be both due to CeOH and ZrOH species. The spectrum we found is similar to that reported by Daturi et al. for Ce_{0.5}Zr_{0.5}O₂ [75]. Such an absorption is significantly decreased in intensity on the catalyst, suggesting that Pd species interact with or exchange surface hydroxy groups. The hydroxy groups are also strongly decreased on the aged support.

On both fresh catalyst and fresh support a sharp peak is observed at 2340 cm⁻¹ and broad bands are observed in the region 1800–1200 cm⁻¹. These features are due to trapped CO₂ molecules and carbonate ions, both residual of the organic molecule used in the preparation of the support. Trapped CO₂ species decrease in amount (their band decrease in intensity) upon ageing, while carbonates disappear completely. New bands appear, conversely, at 1340 and 1280 cm⁻¹, superimposed to the bands due to residual carbonate species, together with a complex and strong absorption centered at 1000 cm⁻¹, with a shoulder around 1100 cm⁻¹.

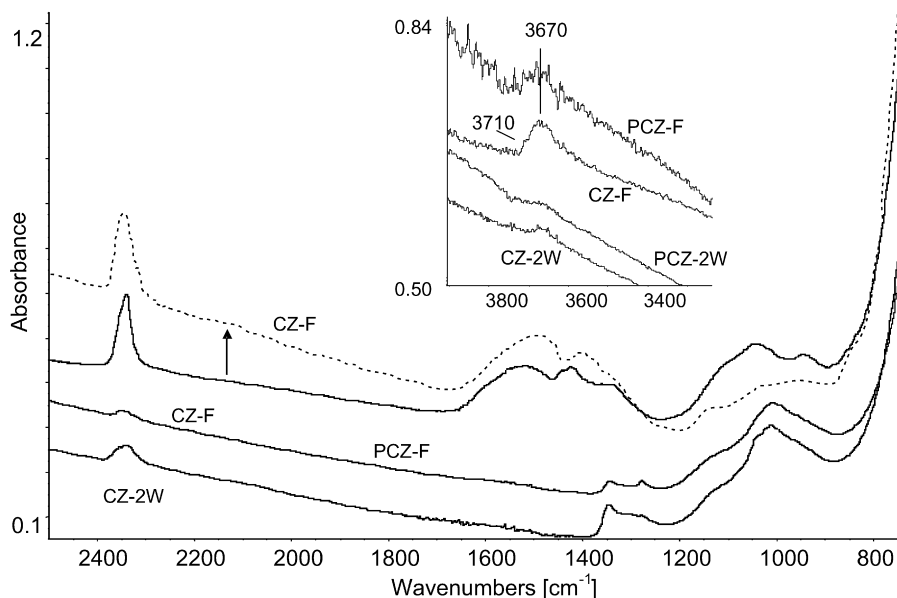


Fig. 4. FT-IR spectra of pure powder pressed disks of the PCZ-F and PCZ-2W catalysts and the corresponding supports (CZ), all after outgassing in vacuum at 400 °C.

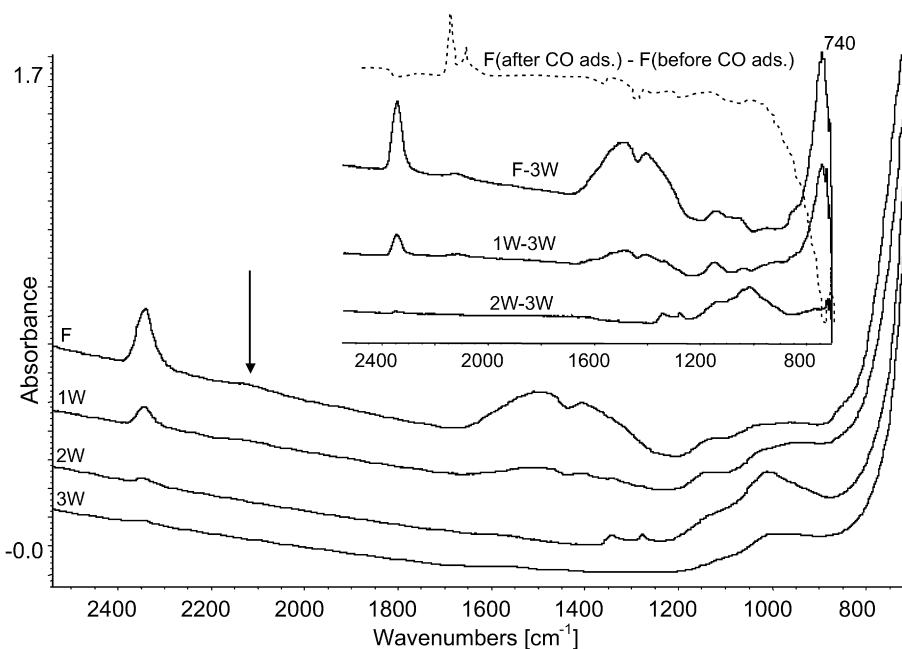


Fig. 5. FT-IR spectra of pure powder pressed disks of the PCZ catalysts, all after outgassing in vacuum at 400 °C, and the corresponding subtractions (in the insert). The broken line in the insert is the subtraction spectrum of sample PCZ-F after-before adsorption of CO.

An absorption tailing to lower frequencies could be also detected. Following literature results [76] these complex bands could be assigned to sulfur containing species. The band around 1340 cm^{-1} is due to S=O stretching mode of a surface (mono-oxo) sulfate species, having some covalent character, while it has been suggested that the band at 1260 cm^{-1} can be assigned to a similar sulfate surface species having different coordination (di-oxo species). An evidence in favor of such assignment came from the behavior of these band which appeared together following 1 week ageing, reached their maximum following 2 weeks ageing then decreased in intensity. This effect could be explained considering surface sulfates formed in a first poisoning step, then diffusing in the bulk. Bands below 1200 cm^{-1} are typically due to S–O stretching modes of ionic sulfates. In particular, bulk (or subsurface) sulfates species over PCZ systems should be characterized by

a complex massif absorption above 1100 cm^{-1} with pronounced shoulder around 1070 and 990 cm^{-1} . The broad absorption tailing towards 900 cm^{-1} , could be assigned to sulfite species, possibly formed by decomposition of sulfate in the present experimental conditions, i.e. heating in vacuum.

In Fig. 5 the overall spectra of the fresh and aged PCZ catalysts are reported. They show again the progressive disappearance of the band of trapped CO_2 and of the surface carbonate species (already fully disappeared in the sample 3W), with the formation of surface and bulk carbonates, that however are largely disappeared again after three weeks ageing, likely due to sintering of the CZ “support.” This suggests bulk sulfates are, more likely “subsurface” sulfates.

In the insert in Fig. 5 are also reported the subtraction spectra, showing the species that disappear after ageing for 3 weeks.

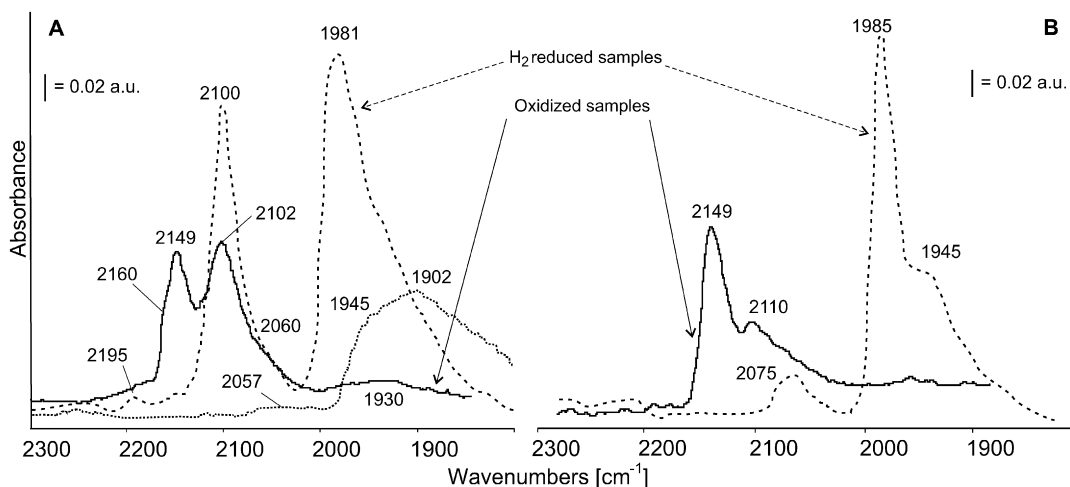


Fig. 6. FT-IR spectra of CO adsorbed on: (A) sample PA1, after previous calcination in air at 400 °C and outgassing at 400 °C (full line), after reduction in H₂ 1 atm at 400 °C (broken line), in contact with CO 10 Torr at –140 °C for 5 min; after reduction in H₂ and outgassing at room temperature (dotted line). (B) sample PA2, after previous calcination in air at 400 °C and outgassing at 400 °C (full line) and after reduction in H₂ 1 atm at 400 °C and outgassing at 400 °C (broken line), in contact with CO 10 Torr at –140 °C for 5 min. The corresponding activated surfaces spectra were subtracted.

It seems interesting to remark that the fresh sample and the sample 1W (which are the most active ones, with similar activity and ability to desorb O₂) show a strong band at 740 cm⁻¹, seen with difficulty in the un-subtracted spectra because they are located near the cut-offs of the samples, where absorption grows very much. This band at 740 cm⁻¹ is also observed when the spectrum of the activated pure support is subtracted from that of the PCZ catalyst (not shown). Thus, this species is present on the catalyst but absent on the support. A tentative assignment of this band can be given taking into account the skeletal spectra of PdO. In this case PdO crystallizes in the so called “cooperite” (or PdS) structure, with space group $P4_2/mmc = D_{4h}^9$, $Z = 2$. In this structure Pd²⁺ ions are in square planar coordination, O²⁻ ions being in tetrahedral coordination. The vibrational (IR and Raman) structure of PdO crystallites has been studied by Kliche [77] and by McBride et al. [78]. PdO gives rise to two IR active and two Raman active modes assigned to stretching of the OPd₄ tetrahedral which are located at 668 cm⁻¹ (A_{2u}, IR), 651 cm⁻¹ (B_{1g}, R), 612 cm⁻¹ (E_u², IR) and 445 cm⁻¹ (E_g, R). Being surface metal–oxygen vibrations usually located at slightly higher frequency than bulk metal–oxygen vibrational modes, it is possible to assign the band at 740 cm⁻¹ to a surface Pd–O mode over our catalyst. This feature could be in some way associated to the active sites of our catalysts. As discussed in the following section, also results from CO adsorption over the fresh catalyst are in agreement with this assignment (inset in Fig. 5, broken line spectrum).

On the other hand, there is no evidence of the peaks of bulk PdO particles (668, 612 cm⁻¹ bands) by IR spectra, suggesting that Pd oxide species are actually dispersed on the support or perhaps very small (as confirmed also by XRD spectra).

Another interesting feature in Fig. 5 is the small absorption at 2120 cm⁻¹, whose intensity decreases upon ageing 1 week down to disappear in the 2W sample. This feature, marked with an arrow in Fig. 5, has been assigned previously to an electronic transition of Ce³⁺ ions [79], thus being evidence of a partially reduced state of the catalyst. It seems interesting to remark that this feature, also observed in the spectrum of the 1W sample, is disappeared in those of 2W and 3W samples. This may be taken as an evidence of an increasingly oxidized state of the catalysts upon deactivation in the O₂-containing stream.

In Fig. 6A the IR spectra of CO adsorbed at low temperature over the PA1 catalyst, taken as a reference, are reported after oxidation and outgassing (full line), and after reduction in H₂ (broken line). The Pd atom surface density in this catalyst is

~5.7 atom nm⁻², i.e. very similar to that of the PCZ-3W sample. The XRD pattern of this catalyst after calcinations (not reported here) shows, together with the features of the γ -Al₂O₃ support, the peaks associated to PdO bulk particles. After reduction, PdO is no more present while Pd metal particles become evident. In the oxidized catalyst spectrum a strong band composed of a main maximum at 2149 cm⁻¹ and a pronounced shoulder at 2160 cm⁻¹ is evident, not anymore observed in the case of the reduced catalyst. This band is certainly due to carbonyl species adsorbed over oxidized Pd centers which are reduced by the treatment in H₂. The position of this band allows its assignment to carbonyls over Pd²⁺ sites [58]. It seems interesting to remark that similar bands (i.e. well above 2130 cm⁻¹) have not been reported during CO oxidation over Pd monocrystals [80,81] and on surface oxides of oxidized Pd nanoparticles. According to Schalow et al. [82], CO should not adsorb over such “surface oxides” covering Pd particles. Consequently, it seems likely that these oxidized Pd species are dispersed on the Al₂O₃ support, more than bulk particles. At higher frequencies, a quite definite, although also weak, band is found at 2195 cm⁻¹, due to CO interacting weakly with Al³⁺ ions on the Al₂O₃ support.

In both oxidized and reduced PA1 surfaces a strong band is found centered very near 2100 cm⁻¹ with an additional component envisaged as a shoulder in the region near 2060 cm⁻¹. The maximum tends to shift in both cases to lower frequencies, down to 2085 cm⁻¹, by outgassing and decreasing CO coverage. These features are quite confidently assigned to terminal carbonyls adsorbed on zerovalent Pd atoms. In agreement with this, CO adsorption on Pd monocrystals shows that terminal carbonyls are found, according to Bradshaw and Hoffmann [83], near 2095 cm⁻¹ on both (111) and (100) planes, while according to Goodmann and coworkers [84,85] this band has been found at 2110 cm⁻¹ on Pd(111) [84], but not on Pd(100) [85]. This depends on the different experimental conditions.

At lower frequencies, only a very weak and broad absorption centered at 1930 cm⁻¹ is found in the case of the oxidized catalyst (Fig. 6A, full line). On the contrary, a very strong band is observed in the case of the reduced catalyst (Fig. 6A, broken line) with a main maximum centered at 1981 cm⁻¹, and a pronounced shoulder near 1900 cm⁻¹. By further outgassing (Fig. 6A, dotted line), the main component decreases fast in intensity and its maximum tend to shift down to 1940 cm⁻¹, while the lower frequency shoulder does not decrease in intensity and becomes predominant at lower CO coverages. The vibrational range of these absorptions

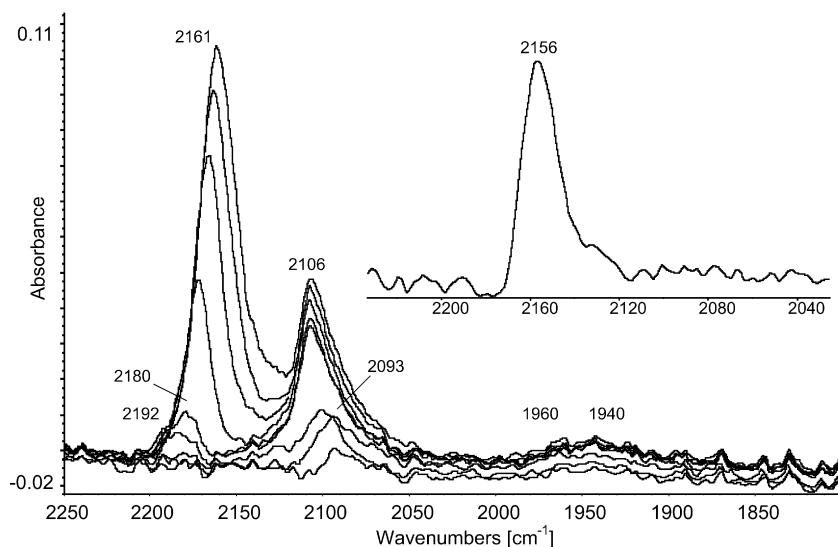


Fig. 7. FT-IR spectra of CO adsorbed on sample PCZ-F, after previous outgassing at 400 °C and contact with CO 10 Torr at -130 °C for 5 min and successive outgassing upon progressive warming until 0 °C (from top to down). The activated spectrum was subtracted. In the insert: the subtraction outgassed at -130 °C, outgassed at -120 °C.

allow their assignment to bridging carbonyls over Pd metal particles. According to Binet et al. [86] the sharper band in the region 1980–1940 cm^{-1} should be assigned to bridging CO on Pd particles exposing a (100) type face while the broader and more strongly bonded band in the 1930–1850 cm^{-1} region should be assigned to bridging CO species adsorbed on Pd particles exposing a (111) type face. This assignment is in agreement with the data arising from CO adsorption over Pd monocrystals [78–81].

The reduction treatment causes the complete disappearance of the bands of oxidized Pd centers (2170–2140 cm^{-1}) and the simultaneous strong growth of the bands of bridging carbonyls on zerovalent Pd. However, also the bands due to terminal carbonyls on zerovalent Pd grow by a factor 2 during reduction. This suggests that few zerovalent Pd particles (or clusters) are already present in the oxidized sample but strongly grow in dimension and number upon reduction.

The spectra of the PA2 catalyst (whose Pd loading is much lower, and also the support area is far higher than for PA1) recorded again after oxidation and outgassing and after reduction in H_2 are reported in Fig. 6B. The Pd atom surface density in this catalyst is ~ 0.78 atom nm^{-2} , i.e., nearly the half with respect to that of the fresh PCZ catalyst, and more than 7 times less than for PA1. XRD patterns of this catalyst too (not reported here), show the presence of small PdO particles in the oxidized state and of Pd metal particles in the reduced one. In the oxidized state a main band at 2149 cm^{-1} is observed, attributed again to carbonyls on Pd^{2+} species highly dispersed on the Al_2O_3 supports. However, in this case the shoulder at 2160 cm^{-1} is not evident. Band at 2160 cm^{-1} (present only on PA1, where Pd loading is far higher and the support area much lower) could be attributed to carbonyl species on more aggregated Pd^{2+} species.

On PA2 it is also possible to find a band at 2110 cm^{-1} , which is however superimposed to a broad absorption tail extending from about 2150 to 2050 cm^{-1} . The peak at 2110 cm^{-1} is attributed to carbonyls of zerovalent Pd. Over this catalyst we do not find, in these conditions, features assigned to bridging carbonyls, suggesting that reduced metal is in fact highly dispersed on PA2.

After reduction in H_2 (Fig. 6B, broken line), again the band at 2149 cm^{-1} disappears, confirming its assignment to carbonyls of oxidized Pd. However, also the feature at 2110 cm^{-1} disappears while a well defined although quite broad peak is now evident at 2075 cm^{-1} . The position of this band allows its assignment to carbonyls on very small Pd particles. On the other hand, a strong

band at 1985 cm^{-1} and a shoulder at 1945 cm^{-1} (likely bridging species on (100) and (111) faces, respectively) confirm the presence of large Pd metallic particles after the reduction treatment. On the other hand, according to a comparison with data concerning CO adsorption on monocrystals, it seems likely that the Pd particles on PA2 reduced sample display more (100) faces than those on PA1, where (111) faces might be more abundant.

The spectra observed on reduced PA1 and PA2 are fully consistent with those reported by several authors for reduced $\text{Pd}/\text{Al}_2\text{O}_3$ catalysts [81,87]. Also the spectra recorded for oxidized sample roughly agree with those reported in the literature [58,60–62]. On the other side, the spectrum found over oxidized samples is quite different from that has been reported by Dellwig et al. [88] for IRAS studies performed during CO oxidation over $\text{Pd}/\text{Al}_2\text{O}_3$. In these conditions, in spite of the presence of O_2 in the atmosphere, only the peaks due to bridging CO species are detectable. It has to be noted, however, that the spectra reported in this study are recorded during reaction at 93 °C. At this temperature, the bands of carbonyls over oxidized Pd centers (2170–2140 cm^{-1}), as well as those due to terminal carbonyls over zerovalent Pd (2120–2080 cm^{-1}), are not observed because the corresponding species are essentially desorbed, i.e., they have a very short lifetime. As discussed elsewhere [59,89], in these conditions, the species which are observed (the bridging carbonyls over Pd metal particles) are likely mostly spectators of the reaction, while those are not observed at all might behave as active species.

The results described above concerning CO adsorption on $\text{Pd}/\text{Al}_2\text{O}_3$ catalysts will be used as references to have information on the state of Pd on low-loading PCZ combustion catalysts. The spectra recorded after low temperature CO adsorption on the fresh PCZ catalyst are shown in Figs. 7 and 8, while the corresponding spectra recorded over pure CZ are shown in Fig. 9.

The main band is detected, in both cases, around 2160 cm^{-1} , its maximum shifting continuously to higher frequencies up to above 2180 cm^{-1} upon outgassing. Also the intensity of this band is very similar in the two cases. Only at room temperature a very weak feature is observed at 2192–2188 cm^{-1} . Being the surface almost completely dehydroxylated, this feature is assigned to CO coordinated over cationic sites, such as Ce^{4+} and Zr^{4+} or Pd^{2+} ions. The discrimination among the different adsorption ionic sites is not straightforward, all of them showing carbonyl complexes at similar wave numbers. However, CO adsorption on Zr^{4+} is likely responsible for the high frequency component of the absorption. In fact,

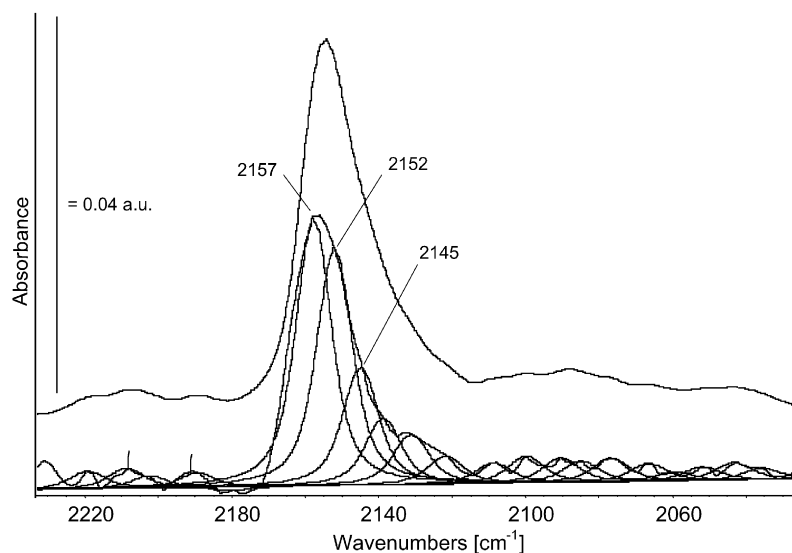


Fig. 8. The subtraction spectrum relative to Fig. 7, after CO adsorption on catalyst PCZ-F outgassed at -130°C , outgassed at -120°C (up) and a deconvolution of the same spectrum (down).

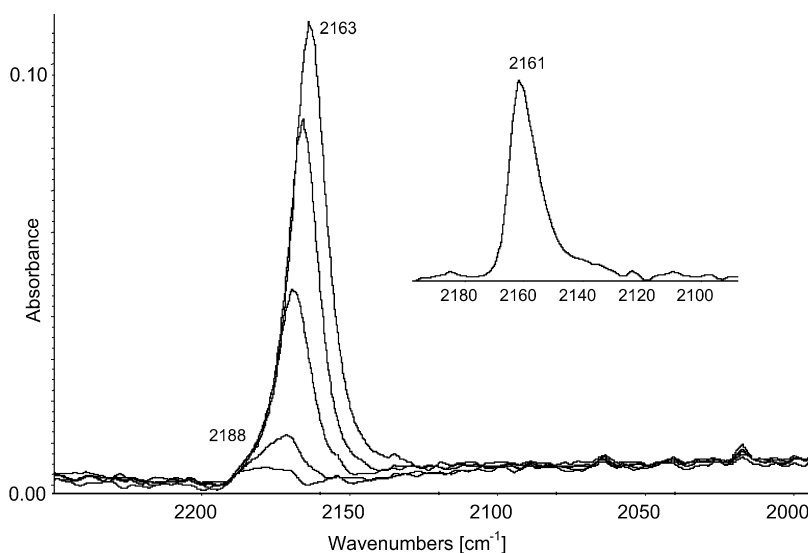


Fig. 9. FT-IR spectra of CO adsorbed on the fresh CZ support, after previous outgassing at 400°C and contact with CO 10 Torr at -130°C for 5 min and successive outgassing upon progressive warming until 0°C (from top to down). The corresponding activated surface spectrum was subtracted. In the insert: the subtraction outgassed at -130°C , outgassed at -120°C .

CO adsorption on ZrO_2 gives usually rise to bands near 2175 and 2190 cm^{-1} [90]. Thus, the main maximum is mostly due to Ce^{4+} carbonyls. In fact, CO adsorption on CeO_2 gives rise to bands in this range [91].

The subtraction for the two samples of the spectra recorded after outgassing at -130 and -120°C is reported in the insert in Figs. 7 and 9, respectively. In the case of the Pd-containing catalysts, the maximum in the subtraction spectrum is observed at 2156 cm^{-1} but several components appear at lower frequency.

A deconvolution of the peak (Fig. 8) shows at least three components in the main band (2157 , 2152 and 2145 cm^{-1}) together with other three weak components in the region 2140 – 2125 cm^{-1} , that could be due to small amounts of carbonyls unreduced Pd centers. In the case of the Pd-free CZ sample, the subtraction spectrum is at distinctly higher frequency, 2161 cm^{-1} , and the lower frequency components appear to be much weaker, if any.

It is possible to remark that upon warming and outgassing, already at -80°C a sharp band at 2345 cm^{-1} starts to grow on the Pd-containing catalyst, superimposed to the band of trapped

CO_2 , cited above. This is not observed in the case of pure CZ. This band is certainly due to CO_2 (asymmetric OCO stretching) adsorbed on the catalyst, being rotational components absent. This indicates that part of CO still bonded in these conditions interacts with strongly oxidizing adsorption sites. This supports the assignment of carbonyl bands absorbing in the region 2160 – 2120 cm^{-1} to CO carbonyl species over oxidized Pd. Consequently, the features observed at 2180 – 2160 cm^{-1} could be identified as Ce^{4+} –CO carbonyl species.

If the spectrum of the fresh catalyst is subtracted from that recorded after CO adsorption, a negative band appears at 745 cm^{-1} (see inset, broken line spectrum in Fig. 5), i.e., just over the peak assigned above to surface Pd–O stretching modes. This suggests that CO adsorption over Pd centers perturbs such modes, likely shifting them to lower frequencies, below the cut-off limit of the sample. This might be taken as a confirmation of the formation of Pd carbonyls.

CO adsorption on unreduced PCZ gives also rise to bands assigned to carbonyl species over Pd metal atoms (Fig. 7). The band

at 2106 cm^{-1} , with a shoulder at 2093 cm^{-1} , is due to linear carbonyls on top of Pd atoms. In parallel, a very weak broad feature is observed split at $1960, 1940\text{ cm}^{-1}$, due to bridging carbonyls. Thus, few quite large and heterogeneous Pd metal particles are present in these conditions, together with dispersed or clustered Pd atoms and ions.

As shown in Fig. 2 and discussed elsewhere [92], after ageing in a real sulfur containing natural gas feed, PCZ catalyst presents a progressive although partial deactivation. The catalyst after this treatment, and, for comparison, also the pure CZ support after the same treatment, were investigated with the same infrared spectroscopic method. Both the catalyst and the support are, after this treatment, contaminated by sulfate species.

The spectrum of CO adsorbed on PCZ-1W sample (Fig. 10A) is very similar to that of the fresh one, according also to its similar catalytic behavior (Fig. 2) and similar O_2 TPD spectrum (Fig. 3). Slight differences are associated to the slightly lower intensity of the bands associated to carbonyls on reduced Pd with respect to those assigned to carbonyls on the support (Ce^{4+} and Zr^{4+} sites) and also those could be attributed to carbonyls on oxidized Pd centers.

The IR spectra of CO adsorbed on PCZ-2W sample (whose catalytic activity is definitely decreased) is much simpler than the previous ones and do not contain any absorption in the region below 2130 cm^{-1} (Fig. 10B). Also, the main band is significantly sharper, losing the absorption shoulder at the highest frequency.

The maximum shifts again upwards by outgassing but only up to 2175 cm^{-1} . This indicates that both Pd metal centers and Zr^{4+} cationic centers are no more available to adsorption of CO. The band observed at $2160\text{--}2175\text{ cm}^{-1}$ is likely due to CO interacting with Ce^{4+} . The loss of Zr^{4+} cationic centers is likely due to the selective poisoning of these sites by sulfates, as reported in the literature for CZ [93]. However, the subtraction spectrum, representing the most labile carbonyl species formed on the surface, is similar in this case to the previous ones, with an evident maximum at 2153 cm^{-1} and a broad component in the region $2150\text{--}2120\text{ cm}^{-1}$. This suggests that very weakly bonded carbonyl species, likely on oxidized Pd centers, still exist on this catalyst.

The spectrum of CO adsorbed on PCZ-3W catalyst (Fig. 10C) is quite similar to that of the 2W sample, confirming the full unavailability of reduced Pd to CO adsorption. The band due to CO bonded on ionic centers is still present but shows that, upon outgassing, these centers are strongly weakened in adsorption strength. Additionally, the broad feature at low frequency extends to a broader and lower frequency range than for the 2W catalyst, in the region $2150\text{--}2050\text{ cm}^{-1}$, and is even more evident here, because of the weakness of the main band. This absorption is assigned again to carbonyls on Pd oxide species.

A comparison of the behavior of the PCZ-2W catalyst respect to the 2 weeks aged CZ support was also performed. The band observed on the aged catalyst is more resistant to outgassing than that observed on the Pd-free sample and, additionally, the oxidation on the catalyst of CO to CO_2 (growth band at 2345 cm^{-1}) is observed at very low temperature. This is shown in Fig. 11 where the spectra of the aged PCZ catalyst is compared with that of the aged CZ support after adsorption of CO at -140°C and warming at -20°C under outgassing. The band of CO_2 grows in this temperature range over the Pd-containing catalyst, showing its still strong oxidizing power.

These data suggest that also oxidized Pd species are actually present on the 2W sample and retain oxidation activity. These species adsorb CO giving rise to carbonyls characterized by a broad band in the region $2160\text{--}2120\text{ cm}^{-1}$ and possibly also participating to the main band in the region $2170\text{--}2150\text{ cm}^{-1}$.

4. Discussion

The data reported here allow a contribution to the interpretation of the behavior of PCZ as catalysts for natural gas combustion. O_2 TPD nicely correlate with CH_4 TPC data showing that ageing results in a decrease in the catalytic activity of the sample which is due to a progressively lowered activity of Pd species to release O_2 , whose full amount is actually not changed. This in spite of the severe loss of total surface area of the samples. On the other hand, the modification to both TPC and TPD activity caused by one week ageing is very small. The 2W sample shows an intermediate behavior while 3 weeks ageing causes a complete change in the behavior. In spite of this, the 3W sample retains catalytic activity with total CH_4 combustion in TPC experiments above 600°C .

O_2 TPD data show O_2 desorption from the fresh catalyst in a temperature range ($430\text{--}550^\circ\text{C}$) typical of O_2 desorption from Pd metal, more than for decomposition of PdO particles. O_2 desorption from the 3W sample, instead, is found just on the typical region of PdO decomposition ($650\text{--}850^\circ\text{C}$).

IR spectra of adsorbed CO show, on the fresh catalyst, the presence of well dispersed reduced Pd metal atoms with few larger Pd metal particles. This is deduced by the intensity of the bands of terminal and bridging CO over zerovalent Pd.

The partially reduced state of this catalyst is also associated to the detection of the weak absorption at 2120 cm^{-1} , due to electronic transition of Ce^{3+} ions. Additionally, the presence at the surface of both Zr and Ce atoms is evident (as expected indeed) together with features that must be assigned to the presence of unreduced Pd ions. These are a weak and broad absorption in the range $2150\text{--}2100\text{ cm}^{-1}$ and also a well defined band in the range $2150\text{--}2160\text{ cm}^{-1}$. Both these features are due to very weakly bonded carbonyl species which are not found on the Pd-free samples.

It is evident that the progressive partial loss of catalytic activity upon ageing corresponds to the total disappearance of the features associated to reduced Pd centers, while the weak features which could be attributed to oxidized Pd centers seem to persist, at least partially, upon ageing and deactivation. TPR data indicate that the amount of reducible Pd oxide species increase upon ageing and deactivation.

The results of the present investigation may be interpreted in relation to recent surface science results reported for Pd nanoparticles supported over different materials. According to Schalow et al. [94] as well as to Dellwig et al. [88], Pd particles grown over ordered Fe_3O_4 and Al_2O_3 substrates, respectively, are constituted by aggregates grown in (111) orientation with an azimuthal alignment with respect to the oxide support. These particles expose (111) facets and a small fraction of (100) facets. The IR spectra of CO adsorbed over such Pd- Al_2O_3 materials [82] are actually very similar to those we report here for CO on our reduced Pd/ Al_2O_3 samples, PA1 and PA2, suggesting that the state of Pd is similar in these cases. Studies of the oxidation of Pd on these materials agree with those reported in the literature for oxidation of Pd single crystals, as discussed by Libuda and Freund [65]. On Pd single crystal studies, it has been shown that O_2 adsorbs dissociatively up to 130°C forming ordered overlayers of chemisorbed O_2 . At higher temperatures (beyond 230°C) the O_2 uptake is far higher and the formation of surface oxides occurs, in parallel with a major reconstruction of the Pd surface. According to Schalow et al. [82], however, two kinds of Pd oxides form in the case of Pd/ Fe_3O_4 surface. Interface Pd oxide first grows at the interface between the metal and the support, later surface oxide grows the more the higher is the reaction temperature. These surface oxides can be dynamically formed and decomposed [91]. Pd metal surface coexists with Pd oxide surface until 330°C , when oxidation of the surface

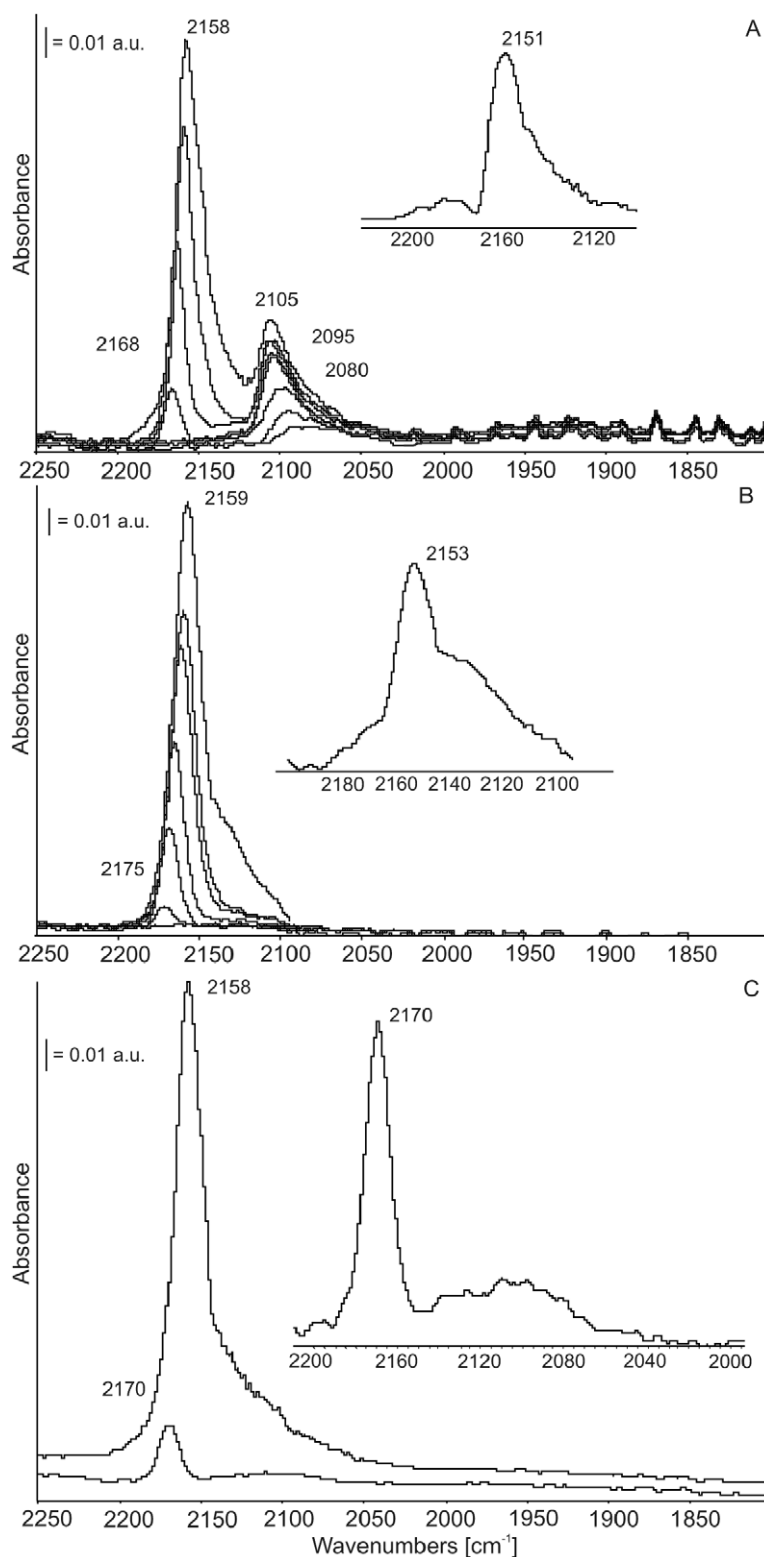


Fig. 10. FT-IR spectra of CO adsorbed on: (A) sample PCZ-1W; (B) sample PCZ-2W after previous outgassing at 400 °C and contact with CO (10 Torr) at –130 °C for 5 min and successive outgassing upon progressive warming up to 0 °C (from top to bottom). Inset: subtraction spectrum [outgassed at –130 °C] – [outgassed at –120 °C]; (C) sample PCZ-3W after previous outgassing at 400 °C and contact with CO (10 Torr) at –130 °C for 5 min and successive outgassing (top) and upon warming up to –60 °C (bottom). Inset: subtraction spectrum [outgassed at –130 °C] – [outgassed at –120 °C]. The corresponding activated surfaces spectra were subtracted.

is complete. It seems also interesting to remark that, according to Schalow et al. [82], surface Pd oxide are not active in adsorbing CO. The picture arising from these studies looks quite the reverse of the proposal of Su et al. [49] who suggested Pd metal to form on top of its oxide.

Taking into account the obtained experimental results together with literature data, in the present most active catalysts (the fresh one and 1W samples), such as also on Pd-containing catalysts for CO oxidation [76,77,84], Pd metal (very small particles or clusters, in this case) and Pd oxide species coexist and likely work synergis-

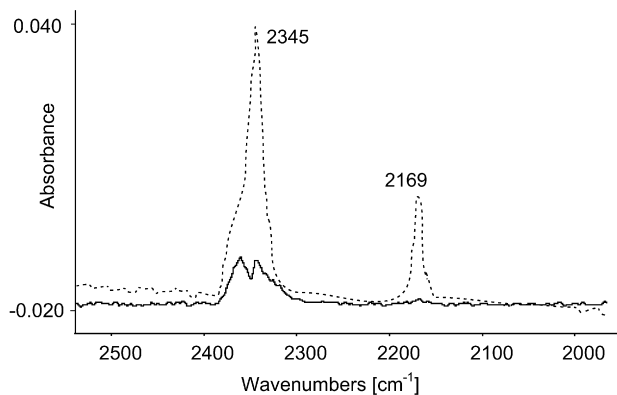


Fig. 11. A comparison of the spectra of the residual species adsorbed on PCZ-2W (broken line) and on the pure support (CZ) aged for 3 weeks (full line) after CO adsorption at -130°C and outgassing at -20°C .

tically. It seems reasonable to suppose that CH_4 activation may be easier on Pd metal, Pd oxide providing O_2 species to form CO_2 .

The deactivation occurring upon the first two weeks of ageing should correspond mainly to the surface oxidation of Pd metal crystals. This oxidation is evident here due to the progressive disappearance, on the 1W and 2W samples, of the features of the reduced Pd centers. In fact, using CO as a surface probe in IR experiments, terminal and bridging carbonyls over zerovalent Pd are observed on the fresh catalyst, while terminal carbonyls over zerovalent Pd are observed on the 1W sample. Both these species are essentially fully disappeared after 2 weeks ageing. This species seem to be also associated to the band observed at 740 cm^{-1} , which could be due to Pd–O stretching for such partially oxidized Pd species.

CO as a probe, according to Schalow et al. [82], should not reveal the results of such a full oxidation of Pd metal, i.e., the presence of such surface oxide phase. Here (working with definitely higher CO pressures compared to Schalow et al. [82]), probably this species is likely responsible for very weak and broad absorption in the range $2150\text{--}2100\text{ cm}^{-1}$, found in all the tested catalysts. The weakness of the adsorption of CO and of its vibrational perturbation, is likely due to the small polarizing power of Pd^{2+} ions and also by their low Lewis acidity, associated to the strong basicity of the oxide ions in PdO_x species.

Both catalytic and O_2 TPD experiments indicate that the situation is deeply modified after 3 weeks ageing. The O_2 TPD curve supports the idea that, in these conditions, species behaving as PdO particles are mostly formed. This results in a definite lowering of catalytic activity in the temperature range below 600°C , which, however, still remains significant. IR spectra for the 3W sample do not detect, indeed, any reduced Pd centers. It seems likely that the broad CO stretching feature detected upon CO adsorption, extending in the range $2130\text{--}2060\text{ cm}^{-1}$ (i.e., in a lower frequency range with respect the less aged catalysts), could be associated to the weak CO adsorption on PdO crystallites.

Dispersed Pd^{2+} species on the oxide support are also observed by IR in this study. They are likely more Lewis acidic and, consequently, give rise to sharper and more evident band in the region $2160\text{--}2140\text{ cm}^{-1}$. Some of these species are present on our catalyst (as they are, certainly, on Pd/ Al_2O_3 samples) but are partly masked by the absorptions of CO on Ce^{4+} and Zr^{4+} ions. These species seem to persist even after ageing. It seems likely that these species, which are certainly stabilized by the interaction with the support, are less active to oxidation (less easily reducible) but may have a role in activating reactant molecules such as hydrocarbons, due to their stronger acidity. In any case, their amount seems to decrease, probably in parallel with sintering of the support.

It seems likely that the progressive oxidation of Pd particles to PdO_x , as well as the coalescence of dispersed Pd oxide species result in fully oxidized PdO_x particles in the 3W sample whose activity is lower. In agreement with this, according to Schalow et al. [82] the activity for CO oxidation of surface Pd oxide is lower than that of Pd metal with chemisorbed O_2 . However, the amount of O_2 stored does not change significantly with ageing, probably because the higher O_2 content of oxidized PdO_x particles is balanced by the O_2 lost by the coalescence of dispersed Pd oxide species. The results here reported and extensively discussed are, in contrast to most of the previous literature on the subject, relative to small Pd loading catalysts (which may find practical industrial application in catalytic combustion), and on their activity at relatively low temperature. In this case, Pd appears to form highly dispersed active species different from bulk Pd and PdO, to which refer most of the previous literature.

If the interpretation of the present data is correct, in the low temperature range $200\text{--}500^{\circ}\text{C}$ (where bulk PdO is more thermodynamically stable with respect to bulk Pd, but probably not with respect to dispersed PdO_x species on the support), the catalysts previously heated at high temperature (where indeed the stable phase is Pd) are mostly constituted by partly oxidized very small Pd metal particles and dispersed Pd oxide species. This situation gives rise to high catalytic activity for CH_4 combustion at low temperature. The progressive oxidation of highly dispersed small Pd particles to PdO_x , as well as the coalescence of dispersed Pd oxide species result in PdO_x particles fully oxidized at least at the surface which are less active (in the low temperature range) with respect to the original catalyst active species. This does not contrast most of the previous literature that showed higher activity in CH_4 combustion at high temperature for large PdO particles with respect to the corresponding large Pd metal particles.

5. Conclusions

A deep chemical characterization study of the surface of 2% Pd powder catalyst supported on $\text{CeO}_2\text{--ZrO}_2$, prepared by solution combustion synthesis, both in fresh and aged status (after accelerated hydro-thermal ageing in presence of SO_2) was carried out. The catalyst is suitable for CH_4 combustion in domestic boilers applications.

The fresh and 1 week-aged catalysts resulted very active in CH_4 combustion, denoting absolutely no deactivation phenomena notwithstanding the aggressive ageing treatment. In both these catalysts, very small Pd metal clusters and Pd oxide species coexist and likely work synergistically: CH_4 activation may be easier on Pd metal, Pd oxide providing O_2 species to form CO_2 .

The deactivation occurred upon the first two weeks of ageing, on 2 and 3 weeks-aged catalysts, probably linked for the most part to the surface oxidation of Pd metal crystals. The progressive oxidation of highly dispersed small Pd particles to PdO_x , as well as the coalescence of dispersed Pd oxide species, resulted, in fact, in PdO_x particles fully oxidized at least at the surface level, which are less active with respect to the species on the catalytic material in its original status.

References

- [1] G. Saracco, I. Cerri, V. Specchia, R. Accornero, Chem. Eng. Sci. 54 (1999) 3599.
- [2] I. Cerri, G. Saracco, V. Specchia, D. Trimis, Chem. Eng. J. 82 (2001) 73.
- [3] D. Ugués, S. Specchia, G. Saracco, Ind. Eng. Chem. Res. 43 (2004) 1990.
- [4] S. Specchia, A. Civera, G. Saracco, Chem. Eng. Sci. 59 (2004) 5091.
- [5] A. Civera, G. Negro, S. Specchia, G. Saracco, V. Specchia, Catal. Today 100 (2005) 275.
- [6] S. Specchia, A. Civera, G. Saracco, V. Specchia, Catal. Today 117 (2006) 427.
- [7] P. Forzatti, G. Groppi, Catal. Today 54 (1999) 165.
- [8] D. Ciuparu, M.R. Lyubovskiy, E. Altman, L.D. Pfefferle, A. Datye, Catal. Rev. Sci. Eng. 44 (2002) 593.

- [9] A. Trovarelli, C. de Leitenburg, M. Boaro, G. Dolcetti, *Catal. Today* 50 (1999) 353.
- [10] S. Colussi, A. Trovarelli, G. Groppi, J. Llorca, *Catal. Commun.* 8 (2007) 1263.
- [11] M.L. Pisarello, V. Milt, M.A. Peralta, E.E. Mirò, *Catal. Today* 75 (2002) 465.
- [12] M. Boaro, M. Vicario, C. de Leitenburg, G. Dolcetti, A. Trovarelli, *Catal. Today* 77 (2003) 407.
- [13] W. Ibashi, G. Groppi, P. Forzatti, *Catal. Today* 83 (2003) 115.
- [14] A. Primavera, A. Trovarelli, C. de Leitenburg, G. Dolcetti, J. Llorca, *Stud. Surf. Sci. Catal.* 119 (1998) 87.
- [15] C.A. Müller, M. Maciejewski, R.A. Koeppl, A. Baiker, *Catal. Today* 47 (1999) 245.
- [16] C. Bozo, N. Guilhaume, E. Garbowski, M. Primet, *Catal. Today* 59 (2000) 33.
- [17] S. Cimino, S. Colonna, S. De Rossi, M. Faticanti, L. Lisi, I. Pettiti, *P. Porta, J. Catal.* 205 (2002) 309.
- [18] S. Larrondo, M.A. Vidal, B. Irigoyen, A.F. Craievich, D.G. Lamas, I.O. Fábregas, G.E. Lascalea, N.E. Walsøe de Reca, N. Amadeo, *Catal. Today* 107–108 (2005) 53.
- [19] C. Bozo, N. Guilhaume, J.-M. Herrmann, *J. Catal.* 203 (2001) 393.
- [20] G. Pecchi, P. Reyes, R. Zamora, T. Lopez, R. Gomez, *J. Chem. Technol. Biotechnol.* 80 (2004) 268.
- [21] F. Yin, S. Ji, F. Zhao, Z. Zhou, J. Zhu, C. Li, *Stud. Surf. Sci. Catal.* 170 (2007) 1380.
- [22] P. Fornasiero, G. Balducci, J. Kašpar, S. Meriani, R. Di Monte, M. Graziani, *Catal. Today* 29 (1996) 47.
- [23] E.S. Putna, J.M. Vohs, R.J. Gorte, G.W. Graham, *Catal. Lett.* 54 (1998) 17.
- [24] J. Kašpar, P. Fornasiero, M. Graziani, *Catal. Today* 50 (1999) 285.
- [25] G.W. Graham, H.-W. Jen, R.W. McCabe, A.M. Straccia, L.P. Haack, *Catal. Lett.* 67 (2000) 99.
- [26] P. Fornasiero, R. Di Monte, T. Montini, J. Kašpar, M. Graziani, *Stud. Surf. Sci. Catal.* 130 (2000) 1355.
- [27] E. Mamontov, R. Brezny, M. Koranne, T. Egami, *J. Phys. Chem. B* 107 (2003) 13007.
- [28] R. Rajasree, J.H.B.J. Hoebink, J.C. Schouten, *J. Catal.* 223 (2004) 36.
- [29] N. Hickey, P. Fornasiero, R. Di Monte, J. Kašpar, J.R. González-Velasco, M.A. Gutiérrez-Ortiz, M.P. González-Marcos, J.M. Gatica, S. Bernal, *Chem. Commun.* 2 (2004) 196.
- [30] P. Palmisano, N. Russo, P. Fino, D. Fino, C. Badini, *Appl. Catal. B Environ.* 69 (2006) 85.
- [31] I. Atribak, A. Bueno-López, A. García-García, *J. Catal.* 259 (2008) 123.
- [32] N. Hosseinpour, A.A. Khodadadi, Y. Mortazavi, A. Bazaryari, *Appl. Catal. A Gen.* 353 (2009) 271.
- [33] R. Di Monte, J. Kašpar, P. Fornasiero, A. Ferrero, G. Gubitosa, M. Graziani, *Stud. Surf. Sci. Catal.* 116 (1998) 559.
- [34] L.F. Chen, G. González, J.A. Wang, L.E. Noreña, A. Toledo, S. Castillo, M. Morán-Pineda, *Appl. Surf. Sci.* 243 (2005) 319.
- [35] C. Thomas, O. Gorce, C. Fontaine, J.-M. Krafft, F. Villain, G. Djéga-Mariadassou, *Appl. Catal. B Environ.* 63 (2006) 201.
- [36] Y. Liu, T. Hayakawa, T. Ishii, M. Kumagai, H. Yasuda, K. Suzuki, S. Hamakawa, K. Murata, *Appl. Catal. A Gen.* 210 (2001) 301.
- [37] Z. Leihong, Z. Qingbao, L. Mengfei, T. Botao, X. Yunlong, *J. Rare Earths* 25 (2007) 715.
- [38] C.F. Cullis, B.M. Willatt, *J. Catal.* 83 (1983) 279.
- [39] R.F. Hicks, H. Qi, M.L. Yang, R.G. Lee, *J. Catal.* 122 (1990) 280.
- [40] R.F. Hicks, H. Qi, M.L. Yang, R.G. Lee, *J. Catal.* 122 (1990) 295.
- [41] S.H. Oh, P.J. Mitchell, R.M. Siewert, *J. Catal.* 132 (1991) 287.
- [42] S.H. Oh, P.J. Mitchell, *Appl. Catal. B Environ.* 5 (1994) 165.
- [43] R. Burch, F.J. Urbano, *Appl. Catal. A Gen.* 124 (1995) 121.
- [44] P. Forzatti, *Catal. Today* 83 (2003) 3.
- [45] P. Briot, M. Primet, *Appl. Catal.* 68 (1991) 301.
- [46] R.J. Farrauto, J.K. Lampert, M.C. Hobson, E.M. Waterman, *Appl. Catal. B Environ.* 6 (1995) 263.
- [47] J.G. McCarty, *Catal. Today* 26 (1995) 283.
- [48] Y. Ozawa, Y. Tochihara, M. Nagai, S. Omi, *Chem. Eng. Sci.* 58 (2003) 671.
- [49] S.C. Su, J.N. Carstens, A.T. Bell, *J. Catal.* 176 (1998) 125.
- [50] M. Lyubovskiy, L. Pfefferle, *Appl. Catal. A Gen.* 173 (1998) 107.
- [51] M. Lyubovskiy, L. Pfefferle, *Catal. Today* 47 (1999) 29.
- [52] J.S. Werner, *J. Electrochem. Soc.* 114 (1967) 68.
- [53] K. Kleykamp, *Z. Phys. Chem. N.F.* 71 (1970) 142.
- [54] G. Vlaic, R. Di Monte, P. Fornasiero, E. Fonda, J. Kašpar, M. Graziani, *Stud. Surf. Sci. Catal.* 116 (1998) 185.
- [55] P. Fornasiero, J. Kašpar, V. Sergio, M. Graziani, *J. Catal.* 182 (1999) 56.
- [56] N. Hickey, P. Fornasiero, J. Kašpar, J. M. Gatica, S. Bernal, *J. Catal.* 200 (2001) 181.
- [57] P.O. Thevenin, A. Alcalde, L.J. Pettersson, S.G. Järås, J.L.G. Fierro, *J. Catal.* 215 (2003) 78.
- [58] M.A. Vannice, in: J.R. Anderson, M. Boudart (Eds.), *Catalysis, Science and Technology*, vol. 3, Springer-Verlag, New York, 1982, p. 139.
- [59] G. Rupprechter, *Catal. Today* 126 (2007) 3.
- [60] K.I. Hadjiivanov, G.N. Vayssilov, *Adv. Catal.* 47 (2002) 307.
- [61] G. Busca, in: S.D. Jackson, J.S.J. Hargreaves (Eds.), *Metal Oxide Catalysis*, vol. 1, Wiley-VCH, Weinheim, 2008, p. 95.
- [62] K.I. Choi, M.A. Vannice, *J. Catal.* 131 (1991) 36.
- [63] O.S. Alexeev, S. Krishnamoorthy, C. Jensen, M.S. Ziebarth, G. Yaluri, T.G. Ruberie, M.D. Amiridis, *Catal. Today* 127 (2007) 189.
- [64] V. Sanchez-Escribano, L. Arrighi, P. Riani, R. Marazza, G. Busca, *Langmuir* 22 (2006) 9214.
- [65] J. Libuda, H.-J. Freund, *Surf. Sci. Rep.* 57 (2005) 157.
- [66] B. Huber, P. Koskinen, H. Häkkinen, M. Moseler, *Nat. Mater.* 5 (2006) 44.
- [67] S. Specchia, M.A. Ahumada Iribarra, P. Palmisano, G. Saracco, V. Specchia, *Ind. Eng. Chem. Res.* 46 (2007) 6666.
- [68] M.F.M. Zwinkels, S.G. Järås, P. Govin Menon, T.A. Griffin, *Catal. Rev. Sci. Eng.* 35 (1993) 319.
- [69] A. Civera, M. Pavese, G. Saracco, V. Specchia, *Catal. Today* 83 (2003) 199.
- [70] I. Rosso, S. Fiorilli, B. Onida, G. Saracco, E. Garrone, *J. Phys. Chem. B* 106 (2002) 11980.
- [71] D. Klvana, J. Delval, J. Kirchnerova, J. Chaouri, *Appl. Catal. A Gen.* 165 (1997) 171.
- [72] V. Sánchez Escribano, E. Fernández López, M. Panizza, C. Resini, J.M. Gallardo Amores, G. Busca, *Solid State Sci.* 5 (2003) 1369.
- [73] H.H. Kan, R.B. Shumbera, J.F. Weaver, *Surf. Sci.* 602 (2008) 1337.
- [74] K.-H. Jacob, E. Knözinger, S. Benier, *J. Mater. Chem.* 3 (1993) 651.
- [75] M. Daturi, E. Finocchio, C. Binet, J.C. Lavalley, F. Fally, V. Perrichon, *J. Phys. Chem. B* 103 (1999) 4884.
- [76] M. Waquif, P. Bazin, O. Saur, J.C. Lavalley, G. Blanchard, O. Touret, *Appl. Catal. B Environ.* 11 (1997) 193.
- [77] G. Kliche, *Infrared Phys.* 25 (1985) 381.
- [78] J.R. McBride, K.C. Hass, W.H. Weber, *Phys. Rev. B* 44 (1991) 5016.
- [79] E. Finocchio, M. Daturi, C. Binet, J.C. Lavalley, G. Blanchard, *Catal. Today* 52 (1999) 53.
- [80] J. Szanyi, D.W. Goodman, *J. Phys. Chem.* 98 (1994) 2972.
- [81] J. Szanyi, W.K. Kuhn, D.W. Goodman, *J. Phys. Chem.* 98 (1994) 2978.
- [82] T. Schalow, B. Brandt, M. Laurin, S. Schaueremann, S. Guimond, H. Kuhlenbeck, J. Libuda, H.-J. Freund, *Surf. Sci.* 600 (2006) 2528.
- [83] A.M. Bradshaw, F.M. Hoffmann, *Surf. Sci.* 72 (1978) 513.
- [84] W.K. Kuhn, J. Szanyi, D.W. Goodman, *Surf. Sci.* 274 (1992) L611.
- [85] J. Szanyi, W.K. Kung, D.W. Goodman, *J. Vac. Sci. Technol. A* 11 (1993) 1969.
- [86] C. Binet, A. Jodi, J.C. Lavalley, *J. Chem. Phys.* 86 (1989) 451.
- [87] K. Wolter, O. Seifert, J. Libuda, H. Kuhlenbeck, M. Baumer, H.-J. Freund, *Surf. Sci.* 404 (1998) 428.
- [88] T. Dellwig, J. Hartmann, J. Libuda, I. Meusel, G. Rupprechter, H. Unterhalt, H.-J. Freund, *J. Mol. Catal. A Chem.* 162 (2000) 51.
- [89] G. Busca, *Catal. Today* 27 (1996) 457.
- [90] C. Morterra, G. Cerrato, S. Di Ciero, *Appl. Surf. Sci.* 126 (1998) 107.
- [91] C. Binet, M. Daturi, J.C. Lavalley, *Catal. Today* 50 (1999) 207.
- [92] S. Specchia, E. Finocchio, G. Busca, G. Saracco, V. Specchia, *Catal. Today*, in press, DOI: 10.1016/j.cattod.2008.10.035 (2008).
- [93] P. Bazin, O. Saur, J.C. Lavalley, A.M. Le Govic, G. Blanchard, *Stud. Surf. Sci. Catal.* 116 (1998) 571.
- [94] T. Schalow, B. Brandt, M. Laurin, S. Schaueremann, J. Libuda, H.-J. Freund, *J. Catal.* 242 (2006) 58.